Remote Sensing-Based Temporal Analysis of Aletsch Glacier Retreat (1990–2020)

Andrija Krtalić[1][a], Ana Kuveždić Divjak[1][b] and Kristina Zeman Šteković[2]
[1] *University of Zagreb Faculty of Geodesy, Kačićeva 26, Zagreb, Croatia*
[2]
{andrija.krtalic, ana.kuvezdic.divjak}@geof.unizg.hr, kristina.zmn@gmail.com

Keywords: Glacier, Remote Sensing, Climate Changes, Sentinel 2, Landsat 5.

Abstract: Glaciers represent an important component of the cryosphere and are among the most sensitive indicators of climate change and global warming. Over recent decades, climate change has significantly accelerated glacier retreat, prompting the development of various monitoring methods, such as the Glacier Monitoring in Switzerland (GLAMOS) program. Key parameters for understanding glacier dynamics include changes in mass balance, length, surface area, and snow accumulation, all of which are closely tied to climatic variations. These changes manifest as alterations in glacier morphology and mass, resulting in notable retreat compared to previous decades when such trends were less pronounced. This study focuses on analysing changes in the Great Aletsch Glacier, the largest glacier in the Alps, over the period 1990–2020 using remote sensing data/techniques. Automated glacier detection and mapping methods were applied, utilizing optical satellite data from Sentinel-2 and Landsat-5 missions. Glacier extents were delineated and analysed over the 30-year period, integrating satellite-derived estimates with official GLAMOS data and climatological records from the MeteoSwiss agency. The results reveal a reduction of approximately 5.2% in the surface area of the Great Aletsch Glacier, providing valuable insights into the glacier's response to ongoing climate change.

1 INTRODUCTION

Glaciers are massive, permanent ice bodies formed over centuries through the accumulation and compaction of snow into dense ice masses, constituting a critical component of the cryosphere (Hock and Truffer, 2024, Haeberli et al., 2007). While most glaciers are concentrated in polar regions, they are also found in temperate and tropical latitudes at higher altitudes, where they play a crucial role in sustaining human activities. Glaciers in these regions act as vital freshwater reservoirs, support agricultural practices, and often serve as significant attractions for tourism.

On a global scale, glaciers are widely recognized as one of the most visible and sensitive indicators of climate change (Hock and Truffer, 2024); Winsvold et al., 2016). This is particularly evident in alpine and tropical glaciers, which are especially vulnerable to climatic fluctuations. These glaciers are critical for local water resources and human activities, yet they have experienced significant retreat over recent decades due to global warming. To address this, numerous glacier monitoring programs have been established, including Glacier Monitoring in Switzerland (GLAMOS, 2025). Key glacier parameters, such as changes in mass, length, area, and snow cover, are directly linked to climatic variations, with glacier length often responding to climate change after a time lag (Nie et al., 2024, Pandey and Venkataraman, 2012).

Given the importance of glaciers and the potential hazards associated with their retreat, international monitoring initiatives have been developed. Programs such as the World Glacier Monitoring Service (WGMS), Global Land Ice Measurements from Space (GLIMS), the Randolph Glacier Inventory (RGI), GLAMOS, and the Global Terrestrial Network for Glaciers (GTN-G) provide critical insights into the status and dynamics of glaciers worldwide.

[a] https://orcid.org/0000-0002-9441-0179
[b] https://orcid.org/0000-0003-1059-8395

Krtalić, A., Divjak, A. K. and Šteković, K. Z.
Remote Sensing-Based Temporal Analysis of Aletsch Glacier Retreat (1990–2020).
DOI: 10.5220/0013481100003935

In *Proceedings of the 11th International Conference on Geographical Information Systems Theory, Applications and Management (GISTAM 2025)*, pages 253-263
ISBN: 978-989-758-741-2; ISSN: 2184-500X

Monitoring glaciers poses significant challenges due to their vast scale and the logistical difficulty of collecting in situ data. Consequently, remote sensing has become an essential tool for observing glacier dynamics and detecting changes over time. Remote sensing data/technologies enable the systematic collection of Earth observation data, facilitating the monitoring of temporal and spatial changes in glaciers while also aiding in hazard assessments. The literature identifies four primary remote sensing methodologies for glacier monitoring, categorized based on the type of data used: (1) optical and near-infrared sensor data, (2) thermal infrared sensor data, (3) microwave electromagnetic spectrum data, and (4) synthetic aperture radar (SAR) interferometry (Wen and Wang, 2024).

This study focuses on the use of optical and near-infrared sensor data, specifically from the Landsat 5 satellite system, to analyse surface changes in the Great Aletsch Glacier. By leveraging these methods, the research aims to provide valuable insights into the glacier's temporal dynamics and its response to climatic changes over the last three decades.

2 REMOTE SENSING APPROACHES TO GLACIER MONITORING AND HAZARD ASSESSMENT

Mountain glaciers in tropical and temperate regions are very good indicators of climate change (Burns and Nolin, 2014) and are key resources for drinking water, maintaining agriculture and hydropower, especially in dry seasons. The melting and retreat of glaciers due to global warming leads to the creation and enlargement of glacial lakes, which can pose a significant threat in the form of glacial lake outburst floods (GLOF). Globally, about 15 million people are directly exposed to the impacts of potential GLOFs (Taylor, Robinson, Dunning, 2023), and the most endangered areas are Central Asia (India, Pakistan, China), the Andes (Peru), and the European Alpine countries (Switzerland, Austria, Italy), (Emmer et al., 2022).

The continued loss of glacier ice and the expansion of glacial lakes due to climate change, particularly in temperate and tropical densely populated areas, represent a global natural hazard that requires attention to minimize loss of life and destruction of infrastructure. Accordingly, the need to monitor glacier changes has arisen, and global, regional and national monitoring programs of particular importance have been established. The above topic is mostly dealt with by Indian and Pakistani scientists with a focus on Himalayan glacial phenomena (Nie et al., 2024, Pandeyand and Venkataraman, 2016, Shafique et al., 2018), European scientist with a focus on Alps glacials (D'Agatha et al., 2018), and American scientists with a focus on Andean and North American geospace (Bolch and Wheate 2010, Romanov and Gutman, 2000).

Remote sensing-based observations of glacial landforms have proven to be crucial for monitoring changes, as routine in-situ data collection in isolated, hard-to-reach mountainous regions is often very difficult due to large spatial coverage and weather variations (Nie et al., 2024, Wang et al., 2025). There are significant advantages of remote sensing for crisis management, such as continuous observations before and after a certain event, the possibility of integrating a wide range of different complementary sensors and easy integration into geoinformation systems, the use of adaptable and simple algorithms, a significant reduction in fieldwork, archiving and reuse of images. Potential disadvantages, some of which are being addressed and reduced over time, include insufficient spatial and temporal resolution, data incompatibility, technical complexity, the high cost of access to commercial images (sub-meter spatial resolution), and the limited use of optical sensors depending on weather conditions (Kerle and Oppenheimer, 2002).

The first satellite systems for remote sensing had a spatial resolution of 80 m and a small number of spectral channels (Landsat 2). The launch of the Landsat 4 and 5 satellite systems with the Thematic Mapper sensor (Landsat TM), with better spatial and spectral resolution, enabled improved mapping and monitoring of glacial areas. In addition to these data, multisensor satellite data such as MODIS (Rigs et al., 2006), ASTER (Wang et al., 2025), the upcoming Landsat 7 and 8 missions and the new TM (Masek et al., 2006, Shafique et al., 2018), Sentinel 2 (Frank et al., 2016) and also radar images like Sentinel-1. Satellite images are then integrated with global or national meteorological data, digital elevation model (DEM) data, and in situ data using various modelling techniques (Ashraf et al., 2016).

During research, various multispectral channels are most often combined in order to distinguish the desired land cover classes by classification (Dozier, 1989, Rosenthal and Dozier, 1996), useful indices such as the Normalized Difference Vegetation Index (Rouse et al., 1974) and the Normalized Difference Snow Index (Hall, Riggs, 2011) are calculated. and today they are increasingly using machine and deep learning methods (Chu et al., 2022). Many scientists are engaged in measuring various parameters of snow and ice such as the thickness and movement of glaciers using LIDAR (Deems et al., 2013) to estimate the melting of glaciers, or the thickness and volume of snow and ice through aerial photographs (Meyer et al., 2022), and to assess drinking water as well as potential hazards.

The research presented in this paper aims to map and analyse the spatial and temporal changes of the largest Alpine glacier, the Great Aletsch, over a 30-year period (1990–2020). This analysis exclusively utilizes open-access datasets from the Landsat 5 and Sentinel-2 satellite systems, employing selected remote sensing methodologies to provide insights into glacial dynamics and associated hazards.

3 MATHERIALS AND METHODS

3.1 Study Area

The object of the study is the Great Aletsch Glacier, located in the Swiss Alps and representing the largest Alpine ice mass with an area of 78.49 km^2 and a volume of approximately 12 km^3 (data from 2017). The Great Aletsch is one of 1400 Swiss glaciers located in the Alps, and extends between 1650 and 4160 meters above sea level, with a pronounced retreat of the lowest point (GLAMOS, 2025, GLAMOS 1880-2021). The glacier consists of three main tributaries – *Aletschfirn*, *Jungfraufirn and Ewigschneefeld* (Figure 1) which merge at the *Konkordiaplatz* with an ice thickness of 800 - 1000 meters and form a common 'tongue', which extends approximately 15 km to the southwest (GLAMOS).

According to official data (GLAMOS 1880-2021), the glacier area has decreased from 86.62 km^2 in 1976 to 78.48 km^2 (decrease of 9.4%) in 2016. The Great Aletsch Glacier was at its peak around 1860. At that time, it was about 3 km longer than today, and the glacier edge was about 200 m higher in the Aletsch Forest area, and this area stands out today as a belt of relatively young vegetation in the landscape (UNESCO, 2025).

Continuous monitoring of the length of the Great Aletsch Glacier has been taking place since 1870, and a reduction of -3459 meters in length has been recorded in the period 1870-2021. More detailed monitoring was established in 1918 with the installation of the first measuring rod at 3350 m above sea level at Jungfraufirn. The data are publicly available on the GLAMOS website (URL4). Since 1990 (which was chosen as the reference year in this study), the length of the glacier has decreased by -1315.4 m (GLAMOS 2022).

The Greater Aletsch consists of two distinct areas. The first is the accumulation area at higher altitudes, where the annual increase in fresh snow during the winter months is greater than the snowmelt in the summer. The second area is the ablation area below Konkordiaplatz, where the melting of ice is stronger due to higher summer temperatures, and glacier mass is lost in the lower part. It is assumed that this area will see the largest changes in the results of remote sensing data/methods.

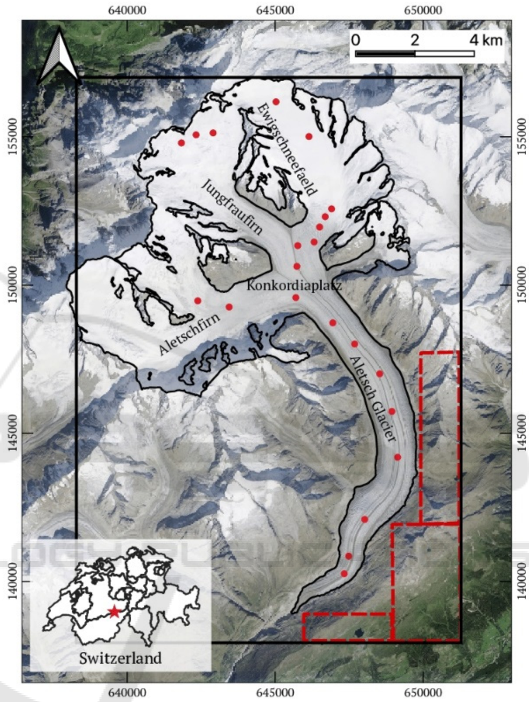

Figure 1: Appearance and position of the main components (Aletschfirn, Jungfraufirn and Ewigschneefeld) of the Great Aletsch Glacier in the Swiss Alps (Source: GLAMOS 1880-2021).

3.2 Climatic Factors Affecting the Great Aletsch Glacier

The development and maintenance of glaciers are largely determined by climatological, orographic and hydrographic features. The average annual temperatures in the upper part of the Great Aletsch Glacier are below freezing, while in the glacier tongue area they are slightly above 0°C (Figure 2a). Another very important indicator for glaciers is the amount of precipitation. Figure 2b shows the relatively dry climate in the glacier tongue, but the highest precipitation in all of Switzerland is measured in the Jungfraujoch glacier accumulation area, which reaches an average of about 3000 mm per year, influenced by precipitation from the north.

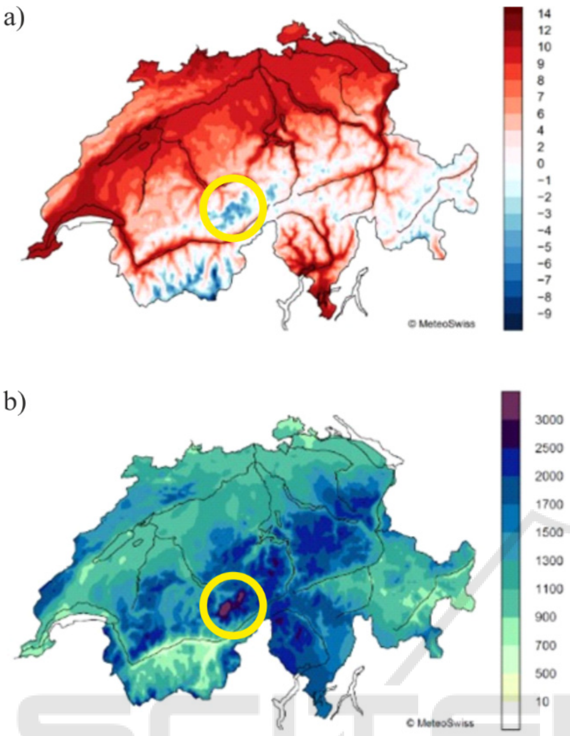

Figure 2: a) Average annual temperature in °C and b) average annual precipitation in mm in Switzerland in the period 1991-2020 (MeteoSwiss, 2025). The location of the Aletsch Glacier is marked with a yellow ellipse.

The amount of snow cover is another important factor for glacier maintenance. Official data from MeteoSwiss show a statistically significant decline in the number of days with fresh snow, as well as in annual fresh snow depths, since the 1960s in many areas of Switzerland, which is accelerating glacier melting (MeteoSwiss, 2025).

Under the influence primarily of temperature and precipitation, the glacier is divided into an area of accumulation (the upper part of the glacier) and ablation, i.e. erosion/landing (the tongue of the glacier), which will later be important for the analysis of the results of this research.

The Jungfraujoch station has been active since 1933 and is located at 3571 m above sea level on the top of the glacier, i.e. in the accumulation area. The climate temperature average for the period 1991-2020 is from -13.3°C in the coldest month of the year (February) to 0.6°C in the warmest month (August). From the annual temperature average monitored until the 1930s, it is evident that the average annual temperature is increasing slightly.

Insolation has been increasing since 1980, and some of the sunniest years occurred after 2000. This development is less pronounced in areas with higher altitudes, namely alpine areas.

3.3 Input Data and Methods

All data and software used for the realization of this research are publicly available and free of charge. QGIS, version 3.28, with the Semi-Automatic Classification (SCP) plugin was used as the primary software for the realization of the work.

3.3.1 Landsat 5 and Sentinel-2 Data

This research is based on the use of images from the Landsat 5 (launched in 1984) and Sentinel-2 (launched in 2015). The study used only images from the Landsat 5 satellite system, in order to use data from the same sensor for the entire time period. Exceptionally, images from the Sentinel-2 satellite system (launched in 2015) were used due to better spatial resolution. The period for which Landsat 5 data is available is 1984-2012, and for Sentinel-2 from 2015 to 2020. Landsat 5 carries the passive sensors Multi-Spectral Scanner (MSS) and Thematic Mapper (TM) and orbits at an altitude of approximately 705 km with a temporal resolution of 16 days. The TM sensor data were used, whose spatial resolution per multispectral channel is 30 m. Sentinel-2A and Sentinel-2B (launched in 2017) are equipped with optical-electronic multispectral sensors (MSI) that create a set of 13 spectral channels (image): 4 channels with a spatial resolution of 10 m, 6 channels with a spatial resolution of 20 m and 3 channels with a spatial resolution of 60 m. Sentinel-2A and Sentinel-2B provide a temporal resolution of 5 days, and a radiometric resolution of 12 bits. The images are available in L1C and L2A processing modes, with the L2A product being fully atmospherically corrected, and the images with this level of processing were used in this work.

For both systems, L2/L2A preprocessing level images were downloaded in GEOtiff format. Satellite systems and dates when the images were created:

- Landsat 5 - 18/08/1990, Scene cloud cover: 4%,
- Landsat 5 - 20/08/2000, Scene cloud cover: 11%,
- Landsat 5 - 09/08/2010, Scene cloud cover: 12%
- Sentinel-2 -07/08/2020, Scene cloud cover: 0.5%

3.3.2 Glamos Data

Glacier Monitoring in Switzerland (GLAMOS) is a glacier monitoring program in Switzerland that systematically documents and monitors long-term changes in glaciers in the Swiss Alps. GLAMOS is jointly managed by ETH Zurich and the Universities of Freiburg and Zurich and the CC Cryospheric Commission. The GLAMOS database contains basic data and facts on more than 1,400 Swiss glaciers covering an area of 641 km2, as well as inventories/databases on changes in glacier length, mass, volume, etc. The inventories contain representations of the outer edges, surfaces and debris covers of all Swiss glaciers.

For the purposes of this work, data on inventories from 1976 (Glacier Inventory, 1976), 2010 (Glacier Inventory, 2010) and 2016 (Glacier Inventory, 2016) and 2022 (GLAMOS, 2022) were downloaded in order to create a mask. with glacier boundaries for cutting individual rasters and for accuracy control. The downloaded data were used in the QGIS software as a shapefile, and were further processed.

The GLAMOS Glacier Inventory data for the years 1976, 2010, 2016 and 2022 were downloaded in a form suitable for processing in QGIS software, i.e. as shapefiles with associated formats (shp, shx, qpj, prj, dbf, cpg).

3.3.3 Copernicus DEM

Digital Elevation Model (DEM) used as a basis for display and analysis of results. The DEM (DEM GLO-30 Public, 2021) was downloaded from the Copernicus Global Digital Elevation Model platform through the OpenTopography portal. The required area is downloaded in the form of GeoTIFF format with 30 m spatial resolution. Through the QGIS software, a hypsometric display with shading and color scale was created for a realistic display.

3.3.4 Input Data Transformation

The downloaded data had different reference systems and datums (Table 1). Therefore, it was necessary to transform all input data into a single project geodetic datum and coordinate system so that the data could be combined. GLAMOS databases store data in the system used in Switzerland and Liechtenstein, while DEM raster data, as well as satellite images, were downloaded in global systems. Finally, the EPSG code 3857 Pseudo Mercator system, which is most commonly used for applications such as Google Maps, OpenStreetMap, ArcGIS, ESRI, was chosen for the research so that the analysis results could be verified with real images widely available to the public (Google maps, etc.).

Table 1: Reference systems of input data in research.

Downloaded data	GLAMOS 1976, 2010, 2016	Copernicus DEM	Landsat 5 Sentinel-2	Data analysis
EPSG code	2056	4326	32632	3857
CRS	CH1903+	WGS84 GPS	WGS 84 / UTM 32N	WGS 84 Pseudo-Mercator

Further processing of all raster and vector data was performed with EPSG code 3857. Due to their size and the slowness of the processing process, the satellite images were cropped to the area of interest using the SCP tool (Clip option), and Landsat 5 images were resampled to Sentinel-2 spatial resolution. Originally, the Landsat 5 and Sentinel 2 images were in the EPSG 32632 reference system, i.e. WGS84, UTM zone 32N, and all images were cropped to a smaller area, where the glacier is visible.

For further mapping and analysis, a glacier mask was created using the GLAMOS database, with the assumption that publicly available data is of the highest accuracy in demarcating individual glaciers from the Great Aletsch 3b).

3.3.5 Normalized Difference Snow Index

The Normalized Difference Snow Index (NDSI) has been shown in the literature to be a reliable algorithm for mapping glaciers due to the fresh snow that covers most of the surface of each glacier (1). Reflectivity varies by snow and ice category - freshly fallen snow has very high reflectivity in the visible and infrared regions. Firn (granular one-year-old snow) has 25-30% lower reflectivity than fresh snow, and glacial ice has high reflectivity in the blue (0.4–0.5 μm) and green (0.5–0.6 μm) wavelength bands that drop sharply to almost zero in the red (0.6–0.7 μm) band. Debris and debris on the glacier surface significantly reduce reflectivity (Pandey et. al., 2016). This algorithm is commonly used in snow/ice mapping applications as well as glacier monitoring. Pixels with a value greater than 0.0 are considered to contain snow cover (Riggs et al., 2016).

NDSI is calculated according to the formulas:

$$\text{NDSI} = (\text{Green-SWIR}) / (\text{Green+SWIR}) \tag{1}$$

3.3.6 The Normalized Difference Vegetation Index

The normalized difference vegetation index (NDVI) was created in order to later classify the land cover more easily. NDVI (2) is the most used indicator for detecting changes in vegetation cover. NDVI is calculated according to the formulas:

$$NDVI = NIR - RED / NIR + RED \tag{2}$$

3.3.7 Supervised Land Cover Classification

Glacier mapping was conducted through supervised land cover classification of the broader Great Aletsch Glacier region. This analysis utilized satellite imagery from the Landsat 5 system for the years 1990, 2000, and 2010, as well as Sentinel-2 imagery for 2020. Supervised classification, a digital image processing technique, was employed to distinguish land cover types based on their spectral characteristics. The primary goal was to produce a thematic land cover map, specifically isolating the glacier surface from the surrounding rocky terrain and vegetated areas.

For each analysed year, one set of rasters was created and a training set of samples for classification was created. The more "homogeneous" areas of the image belonging to the same land cover class were selected, according to the judgment and experience of the operator. The selection of ROI polygons is facilitated by the application of the NDSI and NDVI indices for spotting and extracting snow and vegetation areas. RGB images created with combinations of channels 5-4-3 for Landsat 5, and 11-7-4 for Sentinel 2 were also used. Such combinations of channels qualitatively distinguish snow from vegetation and the surrounding rocky area.

Based on the selected samples for 1990, land cover classification was performed using three methods: Minimum Distance, Maximum Likelihood (classical approaches), and Random Forest (a machine learning method), implemented through the specialized SCP plugin, for the purpose of examining the most appropriate method. After multiple attempts, the Minimum Distance and Maximum Likelihood methods produced unrealistic results and were therefore excluded from further analysis.

Random Forest (Hansch, 2025) is a classification based on machine learning. More samples result in a longer, but better-quality process because there are more samples on which it "learns" how to create a decision. Patterns are created exclusively by manually drawing polygons for compatibility with SNAP and SCP tools. Random Forest is a special machine learning technique based on iterative and random creation of a decision tree, i.e. a set of rules and conditions that define a class.

First, the input features are defined, in this case spectral bands by selecting samples of individual classes. Random Forest calculates several decision trees based on the following parameters: (1) number of training samples: the number of pixels from the training sample that are randomly used to train the model; 5000 was chosen according to the instructions from the SPC, and (2) number of trees: the number of decision trees; the higher the number of trees, the higher the accuracy of the model. 100 was chosen. The separation of trees is defined according to the principle of the Gini coefficient. A pixel is classified as, for example, class 1 if the majority of decision trees evaluated it as class 1.

The causes were selected along the glacier to represent the entire class of “glaciers”, i.e. different types of glaciers cover such as fresh snow, granular snow and glacial ice. The class contains a very wide range of values because glaciers consist of uneven deposits of different types of snow, ice, debris i.e. moraine material and the like. The class of “rocks” has a uniform, relatively low reflectance across all spectral channels and is marked with a light brown colour. The class of “vegetation” has an increased reflectance around 4.0 µm. The class of “shadows” is separated because without it the rock and glacier classes cannot be properly classified.

4 RESULTS AND ANALYSIS

4.1 NDSI and NDVI

The NDSI was calculated for all weather data sets, and the one for 1990 served as a reference value for comparisons. By analysing the image, it is possible to conclude that the higher pixel values (darker colour) are in the upper, accumulation part of the Great Aletsch Glacier, which has more precipitation, i.e. where snow is retained throughout the year. The lower part of the glacier has lower pixel values (weaker colour) where the snow cover is thinner 3).

Only values above 0.0 are selected and shown in the image. Several “lines” running from Konkordiaplatz along the entire length of the glacier tongue can also be successfully observed, these are moraines – accumulations of sediments of unconsolidated glacial debris, regolith and rocks (debris), sometimes called glacial till. The moraine is distinguished by its appearance and remote sensing methods, but it is an integral part of the glacier.

By analysing the NDVI for 1990, it can be seen that in the area of interest, rock, sand and snow are present to a large extent (values -0.1 - 0.1). Only surfaces with values higher than 0.4 (low vegetation such as mountain grasslands) are highlighted on this display.

4.2 Glacier Mapping

Before analysing the results, only the glacier of interest, the Great Aletsch, was separated from the edges of other, surrounding glaciers. In this way, the analysis focused only on the body of the Great Aletsch glacier, which was the goal of this research. All rasters (NDVIs and classification results using the *Random Forest* method for each year of observation 1990, 2000, 2010 and 2020) were extracted using the mask shown in Figure 6b (in QGIS using the *Extraction raster by mask layer* option). This resulted in multiple polygons (glacier area for each observed year) that were merged into a single multipolygon. Using Field calculator, a new attribute called Area (km^2) was added and the area of the polygon representing the glacier for each observed year was calculated using the expression "area($geometry)/ 1000000". For the sake of a more realistic display of details, smoothing of the outline of the glacier was done because the outer line of the glacier remained square by converting the raster into a vector form. Through the tool Processing Toolbox - QGIS geoalgorithms - Vector Geometry Tools, Smooth geometry was created for each layer for the observed years 1990, 2000, 2010 and 2020.

The final data sets for analysis are represented by 4 vector layers – polygons of the mapped Great Aletsch Glacier in selected years for each of the methods used.

4.3 Results Analysis

The analysis involved a comparison of the mapped glacier area obtained by individual methods, and verifiable real field information and officially available data. The analysis of the mapped areas of the Great Aletsch Glacier obtained by the NDSI calculation methods (Figure 3) and the Random Forest classification method (Figure 4) indicates certain changes in the glacier area in the observed period, i.e. the retreat of the Great Aletsch Glacier in selected years was detected and documented.

According to the results of the NDSI with a set of rasters from: 1990, 2000, 2010 and 2020, a regular glacier retreat is visible, which represents the melting of glaciers in accordance with climate change. There is very little change in the accumulation area, while the pronounced retreat of the glacial mass is most pronounced in the glacier tongue. This can also be well monitored in the cuts of the accumulation area (glacier fans). The glacier surface, especially pronounced in the glacier tongue, was the largest in 1990 and has been continuously decreasing over the 30-year period (Figure 3). The glacier retreat is most pronounced longitudinally and in accordance with the orographic characteristics of the terrain (following the glacier valley).

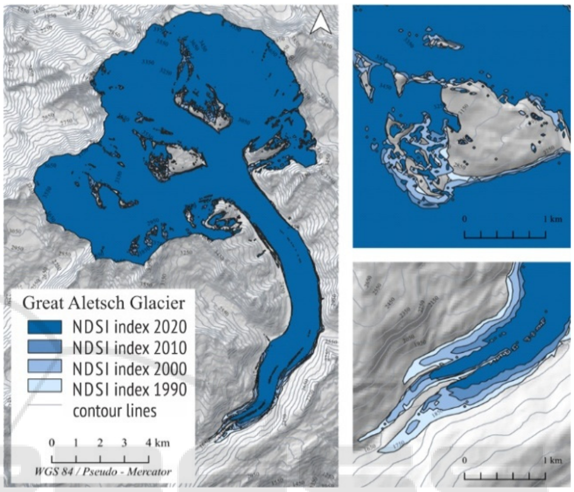

Figure 3. A single view of the all NDSI for the years: 1990, 2000, 2010 and 2020 (left). Enlarged parts of the glacier surface to better see differences by year (right: 'fan' - top right, 'tongue' - bottom right).

The results of the Random Forest classification method (Figure 4) show that the areas in all observed years are smaller and narrower than the glacier areas obtained by calculating the NDSI. Also, the notches in the accumulation area of the glacier (fan) are larger and more pronounced, and the glacier tongue is visibly narrower. The image details mainly show the three observed years, while the glacier surface layer for 1990 barely appears. Namely, the layers are complex in time/chronology and logic dictates that the reduction in the glacier area is followed from the initial observed year when the glacier is largest to the following years when melting is increased and the area is smaller.

However, according to the results of the Random Forest classification, the glacier area for 1990 is smaller than its area for the following two observed years. The irregularity may arise due to insufficient education of the operator performing the classification, inadequate samples for classification, spatial resolution of the satellite image and other technical reasons. It should also be noted that the

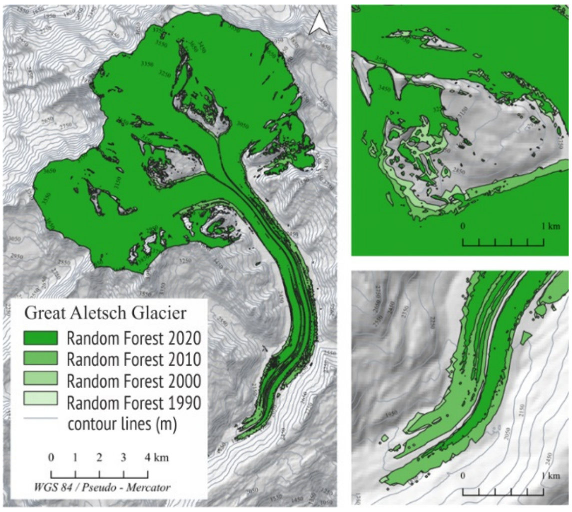

Figure 4. A single view of the all classification results of Random Forest method for the years: 1990, 2000, 2010 and 2020 (left). Enlarged parts of the glacier surface to better see differences by year (right: 'fan' - top right, 'tongue' - bottom right).

classifications for 1990, 2000 and 2010 were carried out with Landsat 5 images with a spatial resolution of 30 m, and for 2020 with Sentinel-2 images with a spatial resolution of 10 m. However, this fact did not affect the calculation of the NDSI.

Still, these irregularities did not affect the spatial patterns and the glacier retreat was still pronounced during the observed years in accordance with the orographic characteristics of the terrain. The retreat can also be monitored on the cuts of the accumulation area (fan). By comparing the results of the two mapping methods, it is possible to see that the classification according to the Random Forest method shows much more pronounced glacier moraines with debris material, i.e. the classification does not systematize these parts as a glacier class but as a non-glacial surface, which further glacier retreat in the observed years. The above reduces the accuracy of mapping glacier surfaces because the moraine is an integral part of the glacier, but consists of accumulations of sediments of unconsolidated glacial debris, regolith and rocks (debris). Several of the previously mentioned reasons reduce the accuracy of the classification method for correctly mapping the Great Aletsch Glacier and lead to the conclusion that the Random Forest method is quite subjective and subject to greater limitations in correctly mapping glaciers than the NDSI calculation method. The area of the Great Aletsch Glacier for 2010, according to the Random Forest classification method, is 76,583 km2, which is a deviation of -1.98% compared to the official GLAMOS data for the same year (78,131 km^2, Table 2).

Table 2: Reference systems of input data in research.

Year	Area (km2) NDSI	Area (km2) Random Forest	Area (km2) GLAMOS
1976			86,628
1990	83.155	73.157	
2000	83.583	75.623	
2010	81.766	76.583	78,131
2016			78,488
2020	78.801	70.459	

A comparison of the implemented glacier mapping methods showed that, in all observed years, the glacier area mapped using the NDSI calculation was significantly larger than that mapped using the Random Forest classification method (Figure 5, Table 2). The largest difference in glacier areas was also observed for 1990, in accordance with the aforementioned irregularity for 1990.

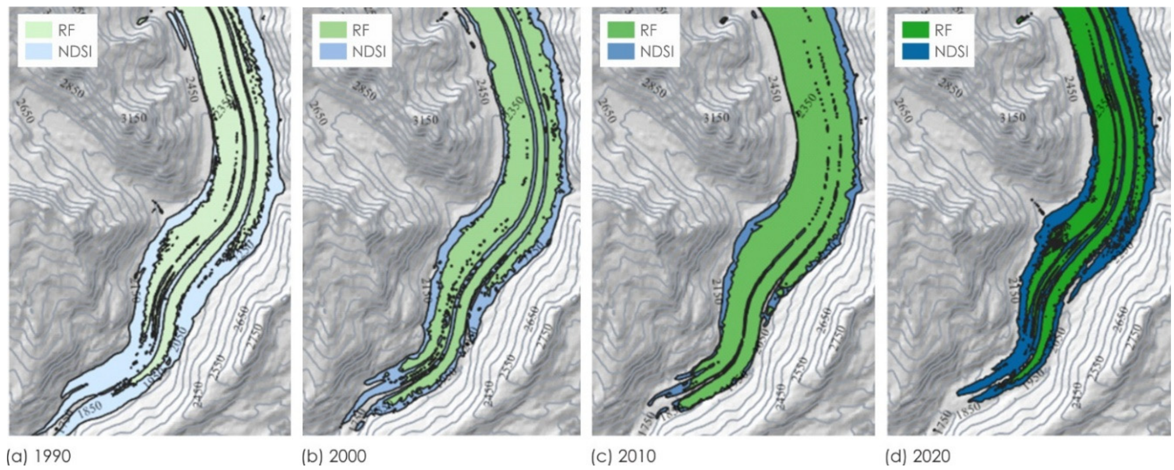

Figure 5. Comparison of the areas of the Great Aletsch Glacier obtained by the NDSI methods (blue tones) and Random Forest classification (green tones) by survey years (a) 1990, (b), 2000, (c) 2010 and (d) 2020.

Table 2 lists the areas of the Great Aletsch Glacier (in km^2) calculated using the NDSI and Random Forest classification methods, as well as the areas of the glaciers from the GLAMOS database for 1976, 2010 and 2016 in order to make the results comparable since reference in situ information could not be collected.

Comparison with actual data from the GLAMOS database for approximately the same period shows that, in general, the NDSI index method provides more reliable and consistent data. In all observed years, the glacier area is larger through the NDSI index compared to the actual data, although the reference mapping boundary was selected as the NDSI value ≥ 0.1 based on viewing satellite images Timelapse Google Earth Engine. The area of the Great Aletsch Glacier for 2010 using the NDSI index method is 81,766 km2, which is a deviation of 4.65% compared to the official GLAMOS data for the same year (78,131 km^2).

The survey did not include the collection of reference field data; therefore, the reference boundary of the mapping was determined arbitrarily and a value of NDSI ≥ 0.1 was selected based on the review of Google Earth Engine satellite images. The assumption is that reference data from the field would contribute to raising the reference limit around NDSI ≥ 0.4, and thus the mapped area of the glacier would be smaller and more consistent with GLAMOS official data.

The analysis determined that the mapping of the Great Aletsch Glacier was more reliable and of higher quality based on the calculation of NDSI with a reference value of NDSI ≥ 0.1. Therefore, these results were linked to the DEM Copernicus GLO-30 digital relief model (30m) to produce a new vector layer and marked hypsometric elevations showing the lowest recorded points of the mapped glacier in the observed years. In 1990, the lowest point of the Great Aletsch Glacier was at approximately 1637 m above sea level, in 2000 at approximately 1670 m, in 2010 at 1735 m above sea level, and in 2020 the retreat of the glacier mass reached 1798 m above sea level (Figure 6).

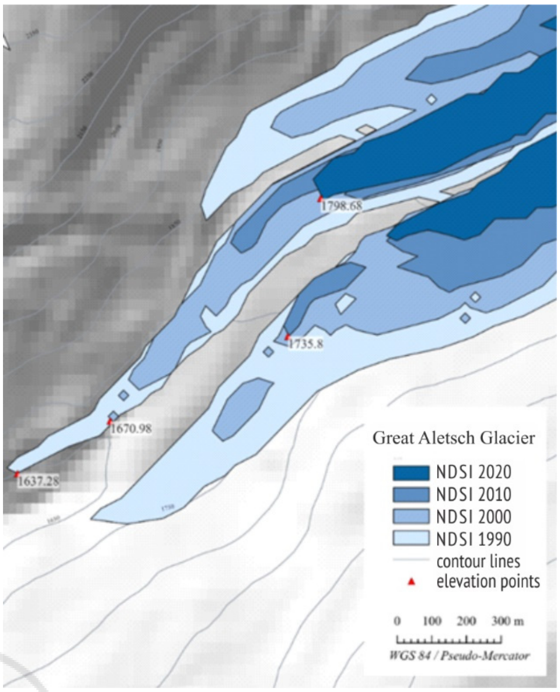

Figure 6. The retreat (melting) of the Great Aletsch Glacier mapped using the NDSI method, with the lowest recorded elevations.

5 CONCLUSIONS

The analysis demonstrated that glacier mapping using the automated calculation of the NDSI index yielded more accurate and reliable results than the Random Forest classification method. While both methods showed some deviations from the GLAMOS reference data—NDSI slightly overestimating glacier areas and Random Forest slightly underestimating them—the NDSI method produced spatial patterns that were more consistent with the orographic characteristics of the terrain. This method allowed for better visualization of glacier retreat, particularly along the tongue of the glacier and in the accumulation area, with fewer mapping errors observed on the surface of the Great Aletsch Glacier.

According to relevant literature, the precise determination of a reference NDSI threshold can significantly enhance the accuracy of glacier surface mapping. In this study, the reference threshold was set to NDSI ≥ 0.1, informed by literature and validated using Google Earth Engine Timelapse imagery. For 2010, the NDSI method estimated the area of the Great Aletsch Glacier at 81.766 km², deviating by 4.65% from the official GLAMOS data (78.131 km²). Conversely, the Random Forest method showed a smaller deviation of -1.98% for the same year. However, visual analysis revealed that the Random Forest method produced more significant mapping errors, while the NDSI approach provided more coherent and reliable results.

The findings suggest that combining these methods (data fusion) has the potential to further improve the accuracy of glacier mapping and monitoring. The NDSI index, in particular, proved to be a simple yet effective methodology for glacier mapping, especially when the reference threshold is verified using reliable in situ data. This study highlights the utility of using free satellite data and open-source software for monitoring changes in the surface area of large glaciers, aligning with the primary goal of demonstrating the feasibility of accessible and cost-effective approaches to glacier monitoring.

REFERENCES

Ashraf, A., Rustam, M., Khan, S.I., Adnan, M., Naz, R, 2016: Chapter 4 Remote Sensing of the Glacial Environment Influenced by Climate Change, Environmental Applications of Remote Sensing, edited by Maged Marghany, 99-129.

Bolch, T., Menounos, B., & Wheate, R. (2010). Landsat-based inventory of glaciers in western Canada, 1985–2005. Remote Sensing of Environment, 114(1), 127–137. doi:10.1016/j.rse.2009.08.015

Burns, P., Nolin, A., 2014: Using atmospherically-corrected Landsat imagery to measure glacier area change in the Cordillera Blanca, Peru from 1987 to 2010, Remote Sensing of environment, 140: 165-178.

Chu, X., Yao, X., Duan, H., Chen, C., Li, J., and Pang, W. 2022: Glacier extraction based on high-spatial-resolution remote-sensing images using a deep-learning approach with attention mechanism, The Cryosphere, 16, 4273–4289, https://doi.org/10.5194/tc-16-4273-2022.

D'Agata, C., Bocchiola, D., Soncini, A., Maragno, D., Smiraglia, C., & Diolaiuti, G. A. (2018). Recent area and volume loss of Alpine glaciers in the Adda River of Italy and their contribution to hydropower production. Cold Regions Science and Technology, 148, 172–184. doi:10.1016/j.coldregions.2017.12.010.

Deems, J. S., Painter, T. H., & Finnegan, D. C. (2013). Lidar measurement of snow depth: a review. Journal of Glaciology, 59 (215), 467–479. doi:10.3189/2013jog12j154.

DEM GLO-30 Public - European Space Agency, Sinergise (2021). Copernicus Global Digital Elevation Model. Distributed by OpenTopography. Accessed: 2023-05-25

Dozier, J., 1989: Spectral signature of alpine snow cover from the Landsat Thematic Mapper. Remote Sensing of Environment, 28, 9–22.

Frank, P., Winsvold, S.H, Kääb, A., Nagler, T., Schwaizer, G, 2016, Glacier remote sensing using Sentinel-2. Part II: Mapping glacier extents and surface facies, and comparison to Landsat 8, Remote Sensing, 8(7):575

GLAMOS - Glacier Monitoring in Switzerland, https://www.glamos.ch/en/#/B36-26, (access on 20/01/2025).

GLAMOS 1880-2021, The Swiss Glaciers 1880-22020/21, Glaciological Reports No 1-142, Yearbooks of the Cryospheric Commission of the Swiss Academy of Sciences (SCNAT), published since 1964 by VAW / ETH Zurich, doi:10.18752/glrep_series

GLAMOS (2022). Swiss Glacier Length Change, release 2022, Glacier Monitoring Switzerland, doi:10.18750/lengthchange.2022.r2022. (access on 20/01/2025).

Glacier Inventory (1976): Müller, F., Caflisch, T. & Müller, G. 1976, Firn und Eis der Schweizer Alpen (Gletscherinventar). Publ. Nr. 57/57a. Geographisches Institut, ETH Zürich, 2 Vols. & Maisch, M., Wipf, A., Denneler, B., Battaglia, J. & Benz, C. 2000, Die Gletscher der Schweizer Alpen: Gletscherhochstand 1850, Aktuelle Vergletscherung, Gletscherschwund-Szenarien. (Schlussbericht NFP 31). 2. Auflage. vdf Hochschulverlag an der ETH Zürich, 373 pp. & Paul, F. 2004, The new Swiss glacier inventory 2000 – application of remote sensing and GIS. PhD Thesis, Department of Geography, University of Zurich, Schriftenreihe Physische Geographie, 52, 210 pp.

Glacier Inventory (2010): Fischer, M., Huss, M., Barboux, C. & Hoelzle, M. 2014, The new Swiss Glacier Inventory SGI2010: relevance of using high-resolution source data in areas dominated by very small glaciers. Arctic, Antarctic, and Alpine Research, 46, 933–945.

Glacier Inventory (2016) - Linsbauer, A., Huss, M., Hodel, E., Bauder, A., Fischer, M., Weidmann, Y., Bärtschi, H. & Schmassmann, E. 2021, The new Swiss Glacier Inventory SGI2016: From a topographical to a glaciological dataset. Frontiers in Earth Science, 22, doi:10.3389/feart.2021.704189.

Hansch, R. Handbook of Random Forests, Theory and Applications for Remote Sensing, Series in Computer Vision: Volume 7, World Scientific Publishing Co Pte Ltd (30 Nov. 2025)

Hock R., Truffer, M. (2024) Glacier hazards: Will they change in the future? Arctic, Antarctic, and Alpine Research, Volume 56, 2024 - Issue 1

Piermattei, L., Zemp, M., Sommer, C., Brun, F., Braun, M. H., Andreassen, L. M., Belart, J. M. C., Berthier, E., Bhattacharya, A., Boehm Vock, L., Bolch, T., Dehecq, A., Dussaillant, I., Falaschi, D., Florentine, C., Floricioiu, D., Ginzler, C., Guillet, G., Hugonnet, R., Huss, M., Kääb, A., King, O., Klug, C., Knuth, F., Krieger, L., La Frenierre, J., McNabb, R., McNeil, C., Prinz, R., Sass, L., Seehaus, T., Shean, D., Treichler, D., Wendt, A., and Yang, R. (2024) Observing glacier elevation changes from spaceborne optical and radar sensors – an inter-comparison experiment using ASTER and TanDEM-X data, The Cryosphere, 18, 3195–3230, https://doi.org/10.5194/tc-18-3195-2024, 2024.

Keshri, A. K., Shukla, A. and Gupta, R. P. (2009): ASTER ratio indices for supraglacial terrain mapping', International Journal of Remote Sensing,30:2,519 — 524

Li, S., Leinss, S., Hajnsek, I. (). Cross-Correlation Stacking for Robust Offset Tracking Using SAR Image Time-Series, IEEE Journal of Selected Topics in Applied Earth Observations and Remote Sensing, Volume: 14, 15 p.

Masek, J.G., Vermote, E.F., Saleous, N., Wolfe, R., Hall, F.G., Huemmrich, F., Gao, F., Kutler, J., and Lim, T.K. (2006). A Landsat surface reflectance data set for North

America, 1990-100, IEEE Geoscience and Remote Sensing Letters. 3:68-72.

MeteoSwis, 2025, Federal Office of Meteorology and Climatology, The climate of Switzerland, https://www.meteoswiss.admin.ch/climate/the-climate-of-switzerland.html, (access on 20/01/2025).

Meyer J, Deems JS, Bormann KJ, Shean DE and Skiles SM (2022) Mapping snow depth and volume at the alpine watershed scale from aerial imagery using Structure from Motion. Front. Earth Sci. 10:989792. doi: 10.3389/feart.2022.989792

Nie, W., Du, Q., Zhang, X., Wang, K., Liu, Y., Wang, Y., Gou, P., Luo, Q., & Zhou, T. (2024). Research on Glacier Changes and Their Influencing Factors in the Yigong Zangbo River Basin of the Tibetan Plateau, China, Based on ICESat-2 Data. *Water*, *16*(18), 2617. https://doi.org/10.3390/w16182617

Pandey, P., Venkataraman, G., 2012: Climate change effect on glacier behavior: A case study from the Himalayas, Earthzine: Climate Consensus.

Pandey, P., Ramanathan, A., Venkataraman, G., 2016: Chapter 5 - Remote sensing of mountain glaciers and related hazards, Environmental Applications of Remote Sensing, edited by Maged Marghany, 131-162

Paul, F., Winsvold, S., Kääb, A., Nagler, T., & Schwaizer, G. (2016). *Glacier Remote Sensing Using Sentinel-2. Part II: Mapping Glacier Extents and Surface Facies, and Comparison to Landsat 8. Remote Sensing, 8(7), 575.* doi:10.3390/rs8070575

Riggs, G. A., Hall, D. K., and Salomonson, V. V., 2006. MODIS Snow Products User Guide. http://modis-snow-ice.gsfc.nasa.gov/sugkc2.html (access on 20/01/2025).

Romanov, P., and Gutman, G., 2000. Automated monitoring of snow cover over North America with multispectral satellite data. Journal of Applied Meteorology, 39, 1866–1880.

Rosenthal, W. and Dozier, J., 1996. Automated mapping of montane snow cover at subpixel resolution from the Landsat Thematic Mapper. Water Resources Research, 32(1), 115–130.

Rouse, J.W., Haas, R.H., Schell, J.A. and Deering, D.W. (1974) Monitoring Vegetation Systems in the Great Plains with ERTS. Third ERTS-1 Symposium NASA, NASA SP-351, Washington DC, 309-317.

Shafique, M., Faiz, B., Bacha, A. S., & Ullah, S. (2018). Evaluating glacier dynamics using temporal remote sensing images: a case study of Hunza Valley, northern Pakistan. Environmental Earth Sciences, 77(5). doi:10.1007/s12665-018-7365-y

UNESCO (2025)- "Swiss Alps Jungfrau-Aletsch". unesco.org. Paris, France: UNESCO World Heritage Centre 1992-2016, UN. 13 December 2001. https://whc.unesco.org/en/list/1037/ (access on 20/01/2025).

Wang, Q.; Yang, Y.; Hu, J.; Zhang, J.; Li, Z.; Wang, Y. (2025). Temporal and Spatial Assessment of Glacier Elevation Change in the Kangri Karpo Region Using ASTER Data from 2000 to 2024. *Atmosphere*, *16*, 110. https://doi.org/10.3390/atmos16010110

Wen M., Wang, T., (2024) Review of SAR imaging geodesy for glacier velocity monitoring, Geodesy and Geodynamics, https://doi.org/10.1016/j.geog.2024.08.004